

# APPLICATION OF HIGH PERFORMANCE MATERIALS AND PROCESSES - ALLOY SYSTEMS

Alan B. Davala, Amie H. Graham, Robert J. Causton  
Hoeganaes Corporation, Cinnaminson, NJ 08077

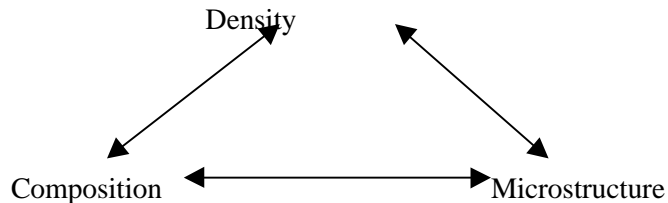
Presented at PM2TEC '98  
International Conference on Powder Metallurgy & Particulate Materials  
May 31 - June 4, 1998 Las Vegas, Nevada USA

## ABSTRACT

Significant advances have been made in the past several years in developing Low alloy materials for highly stressed applications. A review of these material and processing developments will be made. Recent material developments focus on developing high apparent hardness and tensile strength in P/M parts without the need for a secondary quench-hardening operation. The effect of alloy type, alloy content, and cooling rate on hardness and other properties will be discussed.

## BACKGROUND

Continued growth of the P/M industry is very much dependent upon meeting ever increasing performance requirements. The key to continually meeting and surpassing increasing performance targets is to thoroughly understand the density, composition, and microstructure relationships of a given P/M system.



### Density

The role of density in P/M performance is well understood. The benefit of increased density on mechanical performance of P/M parts has been thoroughly investigated over the years. The combination of existing technologies such as double press/double sinter, and new processes like warm compaction with ANCORDERNSE® technology were investigated by Donaldson and Hanejko [1]. Using warm compaction technology they demonstrated that an increase in density of 3.0% resulted in a 30% increase in transverse rupture strength (TRS) of a Distaloy AE based material. Further densification through high temperature sintering resulted in an additional increase of 1.2-% density and an additional 14% increase in TRS. The effect of increased density on ductility measurements, such as tensile elongation and impact properties, is even more pronounced. Understanding how to maximize the density of P/M components is important in pursuing high performance applications.

### Composition and Microstructure

Material composition plays an equally important role in P/M part performance- At a given density, alloying elements that aid in improving the hardenability of the alloy system generally improve the mechanical performance of the system. The role of nickel and molybdenum as alloying elements is well understood and applied in P/M. These alloying elements can be introduced into the iron matrix during the melting step prior to atomization, creating a prealloyed material. Chromium and manganese are limited in use due to their high affinity for oxygen. However, their positive effect on hardenability warrants further investigation in the ongoing development of sinter-hardening materials. The primary benefit of prealloyed P/M materials is uniformity in alloy chemistry within each powder particle, and therefore the entire P/M compact following compaction and sintering. This allows for consistent hardenability throughout the part, providing excellent response to accelerated cooling and/or heat treatment. However, increasing prealloy content generally decreases the powder compressibility and the ability to reach higher density levels.

Nickel and molybdenum particularly have been used in the development of prealloyed powders such as FL-4200 (Ancorsteel® 2000) and FL-4600 (Ancorsteel14600V). These prealloyed powders have been employed for many years in P/M and P/F applications where high performance is required. Even at high compacting pressures, single press density levels are typically limited to 6.8 - 6.9 g/cm<sup>3</sup> due to the compressibility constraints of these materials. However, many automotive and lawn and garden applications requiring wear resistance, i.e. high apparent hardness, have favorably applied these materials with the assistance of sinter-hardening or secondary heat treatment. To further improve the hardenability of these alloys, copper is often admixed to the prealloyed base material. The resultant material is often referred to as a hybrid system. The FLC-4608 composition provides a benchmark material for sinter hardening alloy developments, targeting larger mass P/M components of greater cross-sectional area. Davala, Graham, and Causton investigated the effects of processing conditions on this system [2]. The investigation studied the relationship between post-sintering cooling rates, mechanical performance, and microstructure.

The development of materials with lower prealloyed chemistry content and improved compressibility created additional avenues to improve material performance. The use of molybdenum as the primary alloying element was introduced with FL-4400 (Ancorsteel 85 HP) and Ancorsteel1150 HP. Causton, James, and Fulmer compared the sinter-hardened performance of the FLC-4408 and the FLC-4608 materials [3]. Despite the lower prealloyed content of FLC-4408, an increase in ultimate tensile strength of 50% was achieved over the FLC-4608 under accelerated cooling conditions. The more compressible FLC-4408 material exhibited a 2.5% increase in density when compacted at 45 tsi compared with the FLC-4608.

These important findings demonstrated the importance of understanding composition and density constraints when choosing an alloy and processing system. Causton and Fulmer continued the investigation of the FL-4400 based system by increasing admixed alloy content of copper and nickel to further improve material performance [4]. Ultimate tensile strength and apparent hardness increased directly with increasing martensite content. Through this work a strong understanding of materials, processing, microstructure and mechanical performance was established.

## **INTRODUCTION**

Controlling microstructure with proper material selection and processing conditions offers opportunities to improve mechanical performance [2,3,4]. Specifically, accelerated cooling after sintering will allow for martensitic transformation and an increase in sintered strength and hardness. As discussed above, the benefits of sinter hardening have greatly expanded due to material developments. In addition, developments in accelerated cooling systems have increased cooling capacity making it possible to achieve cooling rates around 2°F/s and a minimum of 85% martensite within large sectioned parts [2].

The current investigation targets alloy development with the following application objectives in mind:

- Apparent hardness greater than 35 HRC with ultimate tensile strength greater than 100,000 psi, when compacted at 40 tsi
- Ultimate tensile strength greater than 120,000 psi with apparent hardness greater than 25 HRC, when compacted at 40 tsi

### Hardness Vs Hardenability

Hardness is the resistance of a metal to permanent (plastic) deformation. The hardness of a metal is measured by forcing an indenter into its surface. For most standard tests, a known load is applied slowly by pressing the indenter into the metal surface being tested. A hardness number is then obtained, which is based on the cross-sectional area or the depth of the impression.

Hardenability provides an indication of the ability of the steel to transform to martensite on cooling. It is the property that determines the depth and distribution of hardness induced by quenching from the austenitic condition [5]. Knowing the chemical analysis and the grain size of a material, the hardenability can be calculated. The calculation is based on the concept of the ideal diameter (D.I.), which is the diameter of a bar that will harden through to the center during an ideal quench. Such a bar, as quenched, will contain approximately 50% martensite in its center. The larger the ideal diameter, the higher the hardenability of the material [6].

A material with high hardenability is one in which austenite is able to transform to martensite without forming pearlite, even when the rate of cooling is rather slow. Optimal sinter-hardening materials would have high hardenability, so that the cooling rates needed to produce large proportions of martensite throughout the section size will be consistently attainable at relatively low cooling rates.

Alloying elements such as molybdenum, nickel, manganese, and chromium promote hardenability in P/M parts. By increasing the hardenability of the material, the parts can be cooled at slower rates and still produce large amounts of martensite. The hardenability characteristics for common alloying elements, taken from ASTM A 255, are shown in Table I.

**Table I: Hardenability Characteristics of Alloys at 0.5% Concentration**

<b>Elements</b>	<b>Hardenability Characteristics.</b>
Chromium	0.318
Manganese	0.426
Molybdenum	0.398
Nickel	0.073

These characteristics show that the hardenability of steels can be controlled through adjustments to the alloy composition [7]. Hardness of a material can be controlled somewhat through adjustments of the carbon content. These predictors are valid for a known carbon content and grain size. Although carbon does not have a big impact on the hardenability of materials, it determines the hardness of the martensite produced. Thus, wear resistant alloys will require high hardenability to promote martensite formation and high carbon content for high hardness. High carbon martensite is brittle, so sinter-hardened parts will require tempering to reduce the risk of premature failure under tensile loads.

### DEVELOPMENT PROGRAM

Design of a sinter-hardening alloy system poses challenges to the powder producer, principally to balance

the need for improved compressibility favored by Low-alloy content with high hardenability favored by higher alloy content. The parts producer also requires a robust material which will provide consistent performance in a wide range of part geometry's and furnace loading that could cause practical cooling rates within parts to vary significantly.

The current investigation studies the effect of alloying content on the hardenability and mechanical performance of new compositions with respect to existing sinter-hardening material systems. This is the first portion of a continuing investigation into new alloy development targeting increased hardenability and density in prealloyed hybrid material systems. The initial part of the program was divided into three phases.

Phase I of this investigation explores many combinations of prealloyed chemistries in search of optimum combinations of hardenability and compressibility under laboratory conditions. In order to properly evaluate potential new prealloyed materials, Phase II was designed to compare new compositions with existing sinter-hardening materials under laboratory conditions. Finally, Phase III was conducted to evaluate the effect of hardenability in a limited number of the materials tested in Phase II. This was accomplished under production sintering conditions, using section size and part mass as a means for hardenability comparison.

## **EXPERIMENTALPROCEDURE**

### *Phase I - Alloy Development*

Based upon the theoretical hardenability calculations, thirteen prealloyed material compositions were chosen for investigation. Five hundred-pound heats of these experimental alloys were atomized and annealed in the Hoeganaes Research and Development process laboratory. The material matrix is shown in Table II.

Chemical analysis was performed on each sample of annealed powder. A premix of each prealloyed sample was prepared with 2 w/o (weight percent) Cu, 0.9 w/o graphite, and 0.75 w/o Acrawax to determine mechanical properties. All samples were prepared and tested according to the appropriate MPIF or ASTM standards [8,9]. Transverse Rupture Strength specimens, nominally 0.25 inches x 0.5 inches x 1.25 inches (6.35 mm x 12.7 mm x 31.75 mm), were compacted at 40 tsi (550 MPa). All samples were sintered under laboratory conditions at 2050°F (1120°C) in hydrogen for 30 minutes at temperature and slow cooled at a rate of 0.50°F/s.

Apparent hardness measurements were performed on the surface of the specimens using a Rockwell hardness tester. Transverse rupture strength was measured according to ASTM B 528.

The materials were then evaluated by comparing their oxygen content, green density, apparent hardness, and transverse rupture strength (TRS). Based on this selection criteria, two prealloyed samples were chosen for further evaluation.

### *Phase II - Alloy Evaluation and Comparison*

To further determine mechanical properties, the two chosen prealloys were premixed with 2 w/o Cu, 0.9 w/o graphite, and 0.75 w/o Acrawax. Four well-known sinter-hardening compositions were also prepared to provide compare five testing references. The prealloyed base powders and premix additions are listed in Table IV.

Green density, green strength, and green expansion were determined from the average of five compacted green strength bars with a nominal size of 0.5 inches x 0.5 inches x 1.25 inches (12.7 mm x 12.7 mm x 31.75 mm). Green strength was determined via a three-point bend test on a Tinius Olsen testing machine with a 5,000-lb. load cell. TRS specimens, 0.25 inches x 0.5 inches x 1.25 inches (6.35 mm x 12.7 mm x 31.75 mm), and dog-bone tensile test pieces were compacted at 30 tsi (415 MPa), 40 tsi (560 MPa), and 50 tsi (690 MPa). All samples were sintered under laboratory conditions at 2050°F (11200C) in hydrogen for 30 minutes at temperature and slow cooled at an approximate rate of 0.54°F/sec.

Apparent hardness measurements were performed on the surface of the specimens using a Rockwell hardness tester. Transverse rupture strength and dimensional change from die size were measured according to ASTM B 528 and B 610. Tensile testing was performed on the dog-bone tensile test pieces. Testing was performed on a 60,000 pound Tinius Olsen universal testing machine at a crosshead speed of 0.1 inches/minute. Elongation values were determined utilizing an extensometer with a range of 0 to 20%. The extensometer was left on to failure.

**Table IV: Existing Sinter-Hardening Materials**

Mix	Base	Ni (w/o)	Mo (w/o)	Cu (w/o)	Ni (w/o)	Graphite (w/o)
SH1	Ancorsteel 85 HP	-	0.85	1.00	2.00	0.90
SH2	Ancorsteel 150 HP	-	1.50	1.00	2.00	0.90
SH3	Ancorsteel 85 HP		0.85	2.00	-	0.70
SH4	Ancorsteel 4600V	1.85	0.55	2.00	-	0.90

*Phase III - Production Sintering*

The two experimental prealloys and four additional sinter-hardening materials were evaluated for hardness response under production processing. To study the effect of production sample size, 1.75-inch diameter test pucks were compacted to a green density of 7.0 g/cm<sup>3</sup>, on a 150-ton Dorst press. Five fixed puck heights were compacted, ranging from 0.25 inches to 1.50 inches, by 0.25 inch increments. The pucks were sintered under production conditions comparing a conventional cooling rate to an accelerated cooling cycle. Test pieces were arranged on 0.250 inch thick ceramic plates typically used to minimize part distortion. The Abbott furnace used in the study was equipped with a VARICOOL® accelerated cooling system, which combines radiant and convection cooling.

The two sintering cycles examined to evaluate the effect of cooling rate on the properties of the selected materials were as follows:

Standard Cycle

Sintering Temperature: 2080°F (1138°C)  
 Belt Speed: 5.0 in/min  
 VARICOOL Setting: OFF (0 Hz)

Sinter-Hardening Cycle

Sintering Temperature: 2080°F (1138°C)  
 Belt Speed: 5.0 in/min  
 VARICOOL Setting: ON (60 Hz)

Under these conditions, the parts were at the sintering temperature for approximately 30 minutes. The sintered parts were stress relieved at 400°F (204°C) in air for 1 hour prior to testing.

Following tempering, apparent hardness measurements were performed on the surface of the pucks using a Rockwell hardness tester. All testing was performed on the Rockwell C scale for comparison purposes. Although some values were below the minimum for this scale, as suggested by ASTM standard E 18 - 94 [9], this single scale was utilized to provide a comparison between a relatively large range of hardness values generated during the tests. The pucks were sectioned, and apparent hardness measurements were taken in the core of each sample.

The pucks were sectioned and prepared for metallographic analysis. Photomicrographs were taken of the microstructures following a 2% nital / 4% picral etch. The martensite content was determined utilizing point count analysis. This analysis technique included the porosity as a portion of the total microstructure. The reported percentages were corrected by eliminating the porosity present in these materials, so that only the metallic portion of the microstructure is considered.

## RESULTS AND DISCUSSION

### *Phase I - Alloy Development*

The test data for the various materials evaluated in Phase I are summarized in Table V. In ferrous powder production, it is desirable to minimize oxygen content and maximize compressibility (density). Materials P1 through P8 all contained mid to high levels of chromium. These materials correspondingly have high levels of oxygen. On average, increasing chromium from Low to mid levels increased the powder oxygen content by 0.1%. Figure 1 demonstrates the relationship between powder oxygen content and green density (compressibility). The materials with high oxygen content exhibited lower green densities. This provided the first criteria for selecting the target-prealloyed materials. Although chromium provides a significant benefit in hardenability, mid to high level chromium containing systems were omitted from Phase II. It was considered that their lower compressibility and higher oxygen content could lead to variation in sintered carbon content, making them less suitable for the present development.

The second set of criteria was based on optimum combinations of sintered hardness and strength. Table V contains surface apparent hardness and TRS values for each material. The initial objective was to select two materials. The first is targeted at maximizing hardness with moderate strength, and the second with moderate hardness and high strength. In the as-sintered state (no temper), TRS decreases with increasing alloy content, while hardness increases. Figures 2 and 3 demonstrate these relationships. Three compositions possess higher properties than the overall trend. Material P11 developed a hardness of 41 HRC, the highest of the materials tested, under laboratory cooling conditions without employing accelerated cooling. Material P9 developed high compressibility and possessed the highest TRS at a 20 HRC under the cooling conditions employed.

Based on both sets of decision criteria described, materials P9, a lean alloy, and P11, a more highly alloyed material, were selected for further evaluation. Several of the other prealloy compositions appear interesting and will be studied further outside of the present investigation.

Figure 4 depicts the apparent hardness results for each material plotted against sintered density. Clearly the new prealloyed material P11 developed the highest apparent hardness. Under fairly slow cooling conditions, P11 is capable of developing an apparent hardness of 36 - 46 HRC in small test samples. SH4 (FLC-4608) exhibited the second highest hardness, ranging from 22 - 28 HRC. The sintered density range

for these two materials appears to be While 2.0 w/o Cu, 0.90 w/o graphite premix additions are common for sinter-hardening materials, the higher dimensional change typically associated with copper additions can present problems. Overall, higher dimensional changes can lead to higher variability. Additionally, high dimensional change results in lower sintered density relative to the green state. Therefore, careful review of dimensional change after sintering is important.

Figure 5 shows the dimensional change results associated with each test material. SH1 and SH2 exhibit the lowest growth due to the 2.0 w/o admixed nickel in these premixes. SH3 and SH4 can be compared more directly with the two experimental alloys because they all contain 2;0 w/o Cu. P9 and P11 exhibit a 40% decrease in dimensional change relative to SH4 (FLC-4608).

Figures 6 and 7 compare the transverse rupture strengths and the ultimate tensile strengths of all of the materials. P9 exhibits the highest TRS values in the 6.64 - 7.02 g/cm<sup>3</sup> sintered density range. At a sintered density of 6.9 g/cm<sup>3</sup>; all materials appear capable of providing a TRS of 120,000 psi or greater when sintered and cooled conventionally.

As mentioned in the procedure, dog-bone tensile specimens were used for this evaluation. Machined round tensile specimens typically produce higher tensile properties relative to dog-bone specimens. This should be considered when reviewing the results. Overall, SH2 provided the highest UTS. This 1.50 w/o molybdenum prealloy admixed with copper and nickel provided the highest sintered density and UTS values in comparison with all materials tested. Following SH2, P9 exhibits the next highest UTS in the 6.64 - 7.02 g/cm<sup>3</sup> sintered density range. Specifically, P9 provides a 19% increase in UTS relative to SH3 and SH4. The UTS of P11 was slightly lower than the observed UTS values for SH3 and SH4. The materials with higher total alloy content are capable of forming higher percentages of martensite. When the amount of martensite exceeds 50%, it is recommended that components should be stress relieved. Tempered martensite will provide higher strength relative to the as-sintered state.

Overall, P9 and P11 both appear to have interesting performance characteristics relative to the existing sinter-hardening materials tested. The lower prealloy content of P9 results in slightly lower hardness than the common sinter-hardening material SH4 (FLC-4608), by approximately 4 HRC at similar sintered densities. However, P9 provides lower dimensional change and higher strength than SH4 in the as-sintered state.

The other developmental prealloy material, P11, provides a significant increase in as sintered hardness over existing sinter-hardening systems at Low cooling rates. Its apparent hardness is higher relative to SH4, by as much as 18 HRC at a given density. The higher prealloyed chemistry was designed to achieve maximum hardness. Its hardness suggested that it transformed almost completely to high carbon martensite on cooling from the sintering temperature. If so, tempering should stress relieve the brittle "as quenched" martensite and increase tensile strength at fracture. This material also appears to offer lower dimensional change relative to SH4.

The two development alloys P9 and P11 along with SH4 were also tested after tempering at 400 °F for 1 hour, in air. Table VII contains these results.

Figure 8 shows the effect of tempering on apparent hardness for all three-alloy systems. The apparent hardness of P9, P11, and SH4 is reduced 2 HRC, 9 HRC, and 6 HRC on average, respectively after tempering Figure 9 shows a dramatic improvement in UTS for all three materials after tempering. P9 increases approximately 16 x 10<sup>3</sup> psi at 6.88 g/cm<sup>3</sup> sintered density after tempering, P11 increases approximately 50 x 10<sup>3</sup> psi at 6.83 g/cm<sup>3</sup> sintered density after tempering, and SH4 increases approximately 27 x 10<sup>3</sup> psi at 6.87 g/cm<sup>3</sup> sintered density after tempering.

These represent an 18%, 70%, and 35% increase in UTS for P9, P11, and SH4, respectively.

A slight increase in sintered density after tempering can be observed in P9 and P11, while a slight decrease in density is seen in SH4. The dramatic improvement in UTS is mainly a function of microstructure enhancement, not density. P11 and SH4 have higher Mn and Ni to Mo ratios and thus most likely have a higher percent of retained austenite. Tempering these structures will decrease hardness while increasing UTS substantially. P9, on the other hand, has a much higher ratio of ferrite stabilizers (Mo) and thus is not significantly changed at this relatively Low tempering temperature.

Table IX contains the results from the standard sintering cycle, representing a slower cooling rate. Under these conditions it is interesting to see that apparent hardness values in excess of 20 HRC can be achieved. Specifically, P11, SH1, and SH4 (FL-4608) exhibit hardness of 19 HRC and greater in the 0.25 inch high pucks. However, only P11 maintains hardness at the 20 HRC level for all section sizes. Figure 10 shows the effect of sample size on apparent hardness for all materials under conventional cooling.

The results from the accelerated cooling cycle appear in Table X. All materials produced higher hardness values under the accelerated cooling conditions. P9, P11, SH2, and SH4 all exhibited 30 HRC or greater in the 0.25 inch high pucks. Figure 11 shows the effect of sample size on apparent hardness for the six materials under accelerated cooling conditions. As the puck height increased, only P11 and SH4 maintained hardness values greater than 30 HRC. P9, SH1, and SH2 maintained hardness in excess of 20 HRC for all sample sizes.

Under standard Jominy end-quench testing, the hardenability of a material is defined by measuring the depth of transformation from a quenched end. This study offers an indication of the hardenability of each material system as a function of section size or part mass under conventional and accelerated cooling conditions. For applications requiring wear resistance, the end user is interested in choosing a material and processing system that will develop the required surface hardness, for specific part geometry. By measuring the core hardness and martensite content of the largest pucks, a relative comparison and ranking of hardenability can be made.

The results from Table XI are plotted in Figures 18 and 19. Figure 18 demonstrates the relationship between apparent hardness and martensite content, while Figure 19 demonstrates the relationship between martensite content and alloy content. Clearly apparent hardness increases as the martensite content increases. The material systems with higher alloy content produce higher amounts of martensite in the core section, indicating a more hardenable material system.

P11 and SH4 exhibited through hardening for all puck sizes under accelerated cooling conditions. This is evident from the high martensite contents and apparent hardness in the core sections. P9 and SH2 develop high hardness values in small section sizes; however the lower hardness in larger section sizes indicates a reduction in hardenability.

## **CONCLUSIONS**

Improved mechanical performance in P/M parts can be achieved through modifications of the density, composition, and microstructure. This continuing research aims to optimize material composition, compressibility, and microstructure through alloy development. Systematic evaluation of various prealloyed chemistries has identified two materials that exhibit enhanced sinter-hardening capability. Benchmark comparisons indicate both developmental materials provide unique combinations of hardenability and strength along with good compactibility. Specifically, two application objectives have been targeted:

- Apparent hardness greater than 35 HRC with ultimate tensile strength greater than 100,000 psi, when compacted at 40 tsi
- Ultimate tensile strength greater than 120,000 psi with apparent hardness greater than 25 HRC, when compacted at 40 tsi

Conclusions from Phase I:

- Green density can be maximized by minimizing powder oxygen content and chromium content.
- In the as-sintered state, apparent hardness is maximized with increasing alloy content.
- Optimization of green density, apparent hardness, and TRS assisted in choosing two new prealloy compositions.

The investigation also confirmed the importance of proper alloy selection to achieve optimum performance characteristics for various process conditions. The methodology of using a slow cooling rate under laboratory conditions ensures the material's responsiveness under the full spectrum of production conditions.

Conclusions from Phase II:

- Developmental prealloyed materials P9 and P11 both appear to have interesting performance characteristics relative to the existing sinter-hardening materials.
- P9 exhibits slightly lower hardness than the common sinter-hardening material SH4 (FLC-4608), by approximately 4 HRC at similar sintered densities. However, P9 provides lower dimensional change and higher strength than SH4 in the as-sintered state.
- P11 provides superior apparent hardness values relative to SH4, by as much as 18 HRC at a given density, along with lower dimensional change.
- Tempering increased strength and decreased apparent hardness in the materials tested. P11 exhibited a 85% larger gain in strength and a 50% lower reduction in apparent hardness compared with SH4 after tempering at 400°F for 1 hour.

The laboratory results from Phase II correlate with Phase III results indicating accelerated cooling capability provides reasonable hardenability response for leaner alloy compositions and increased response for higher alloy compositions.

Conclusions from Phase III:

- The apparent hardness that materials can obtain in a sinter-hardening furnace depends on the hardenability of the material, which is determined by alloy content.
- This production study offered an indication of the hardenability of each material system as a function of section size or part mass under conventional and accelerated cooling conditions.
- P11 and Sd4 exhibited the highest apparent hardness and through hardening capabilities.
- P9 and SH2 reach 30 HRC in small section sizes.
- P11 developed the highest percentage of martensite as measured in the core of the 1.25-inch puck.

This paper presents the initial portions of on-going development of new prealloyed materials for sinter-hardening applications. The research program clearly shows the role of material composition in determining P/M steel performance. By control of alloy composition two new P/M steels were developed

that offer superior combinations of properties to those currently available.

Alloy P11 is a highly hardenable P/M steel that when mixed with 2 w/o copper and 0.9 w/o graphite develops a microstructure of 90% martensite content at the core of 1.25 inch diameter parts. When tempered it possesses excellent strength while maintaining high macrohardness. It should be suitable for producing P/M parts requiring high hardness and wear resistance without a secondary quench-hardening operation.

Alloy P9 is a high compressibility P/M Low-alloy steel. Although it does not develop the extreme apparent hardness of the more highly alloyed P11, it possesses higher as sintered properties and develops excellent strength and apparent hardness when sinter-hardened and tempered.

While this work has focused on alloy development and preliminary qualifications, additional testing is continuing to complement the full commercialization of the products. Specifically, the following topics will be investigated:

- Complete mechanical testing of P9 and P11 compared with SH1, SH2, SH3, and SH4 under the production sinter-hardening conditions employed in Phase III.
- investigation of increased density through double pressing/double sintering and warm compaction of select sinter-hardening systems.
- Investigation of tempering conditions for optimum strength and hardness.
- The exploration of P9 as a base for high performance alloy systems and quench - hardened and tempered systems.

## ACKNOWLEDGMENTS

The authors wish to thank Arthur Rawlings, Ron Fitzpatrick, Steve Mazur, Craig Gamble, Benny Bentcliff, Steve Kotwicz and Jerry Golin for their assistance in preparing, testing and analyzing the samples. We would particularly like to thank the staffs at MascoTech Sintered Components and Abbott Furnace Company for their invaluable expertise and help in performing the sintering.

## REFERENCES

1. Donaldson, i., Hanejko, F.G., "An Investigation into the Effects of processing Methods on the Mechanical Characteristics of High performance Ferrous P/M Materials", *Advances in Powder Metallurgy and Particulate Materials- 1995*, Vol. 2, p. 5-51, Metal Powders industries Federation, Princeton, NJ.
2. Davaia, A.B., Graham, A.H., Causton, R.J., "Effect of Process Conditions Upon Sinter-Hardening Response of FLC-4608 Metedals, *Advances in Powder Metallurgy and Particulate Materials - 1997*, Vol. 2, Part 14, p. 81, Metal Powder Industries Federation, Princeton, NJ.
3. Causton, R.J., James, W.B., Fulmer, J.J., "performance Characteristics of a New Sinter-Hardening Low-Alloy Steel", *Advances in PowderMetallurgy- 1991*, VoL 5, p. 91, Metal Powder Industries Federation, Princeton, NJ.
4. Causton, R.J., Fulmer, J.J., 'Sinter-Hardening Low-Alloy Steels', *Advances in Powder Metallurgy & Particulate Materials - 1992*, VoL 5, p. 17, Metal Powder Industries Federation, Princeton, NJ.
5. Smith, W.F., *Principles of Materials Science & Engineering*, 2nd Edition, McGraw-Hill, Inc., 1990,

p. 270, 502.

6. ASTM standard: A 255-96, 'Test Method for End-Quench Test for Hardenability of Steel', *ASTM Annual Book of Standards 1996*, Vol. 01.05.
7. Causton, R.J., Cimino, T.M., 'High Density Processing of Ct-Mn P/M Steels', *Advances in Powder Metallurgy & Particulate Materials - 1994*, Vol. 5, p. 89, Metal Powder Industries Federation, Princeton, NJ.
8. "Standard Test Methods for Metal Powders and Powder Metallurgy Products", Metal Powder Industries Federation, Princeton, NJ, 1998.
9. "Metals Test Methods and Analytical Procedures", American Society for Testing and Materials, Vol. 03.01, 1995, Philadelphia, PA.

**Table II: Experimental Prealloy Matrix**

Prealloy	Cr	Mn	Ni	Mo
P1	Mid	Mid	Mid	Mid
P2	Mid	Mid	High	High
P3	Mid	Mid	High	Low
P4	Mid	Mid	Low	Low
P5	High	Mid	Low	Low
P6	Mid	Mid	Low	High
P7	Mid	High	Low	Low
P8	Mid	Low	Low	Low
P9	Low	Low	Mid	Low
P10	Low	Mid	High	Low
P11	Low	Mid	High	High
P12	Low	Mid	Mid	Low
P13	Low	Mid	Mid	High

The ranges of the alloy addition are shown in Table III.

**Table III: Alloy Addition Ranges**

Addition	Low (w/o)	Mid (w/o)	High (w/o)
Cr	< 0.25	0.25 - 0.65	> 0.65
Mn	< 0.25	0.25 - 0.65	> 0.65
Ni	< 0.25	0.25 - 0.75	> 0.75
Mo	0.65 - 0.85	0.85 - 1.05	> 1.05

**Table IV: Existing Sinter-Hardening Materials**

Mix	Base	Prealloyed Additions		Premix Additions		
		Ni (w/o)	Mo (w/o)	Cu (w/o)	Ni (w/o)	Graphite (w/o)
SH1	Ancorsteel® 85 HP	--	0.85	1.00	2.00	0.90
SH2	Ancorsteel 150 HP	--	1.50	1.00	2.00	0.90
SH3	Ancorsteel 85 HP	--	0.85	2.00	--	0.70
SH4	Ancorsteel 4600V	1.85	0.55	2.00	--	0.90

Table V: Alloy Evaluation

Prealloy	Oxygen Content (w/o)	Green Density at 40 tsi (g/cm <sup>3</sup> )	Hardness at 40 tsi (HRC)	TRS at 40 tsi (psi x10 <sup>3</sup> )
P1	0.43	6.80	26	131
P2	0.43	6.75	30	126
P3	0.39	6.82	30	142
P4	0.41	6.91	14	149
P5	0.51	6.80	16	134
P6	0.42	6.81	17	139
P7	0.48	6.83	19	130
P8	0.37	6.88	13	147
P9	0.18	6.94	20	158
P10	0.19	6.92	29	110
P11	0.21	6.88	41	111
P12	0.19	6.95	22	139
P13	0.18	6.93	28	128

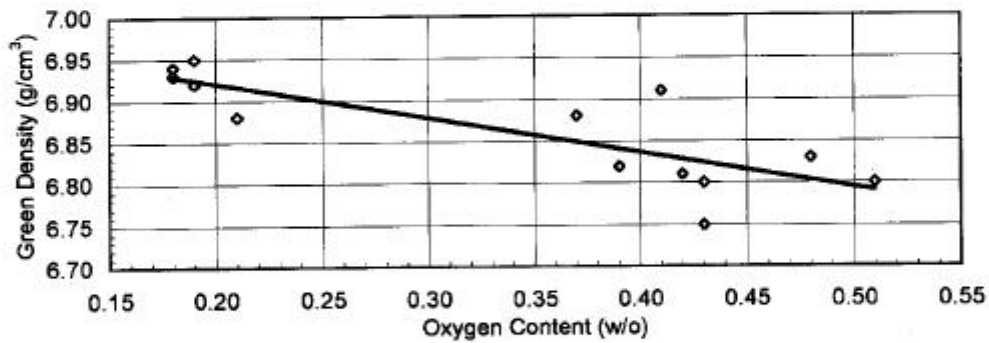


Figure 1: Compressibility at 40 tsi as a Function of Powder Oxygen Content

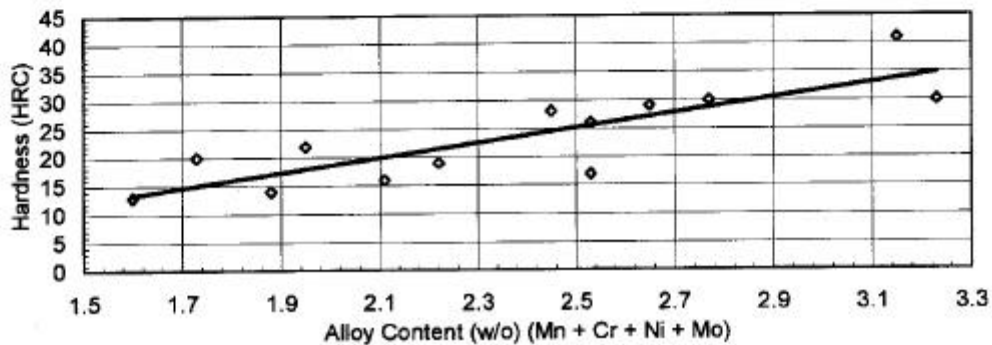
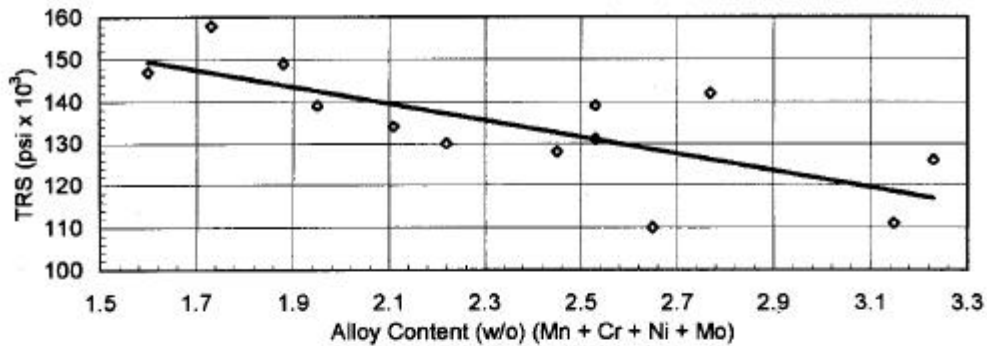


Figure 2: Relationship Between Hardness and Alloy Content, As-Sintered without Temper



**Figure 3: Relationship Between Transverse Rupture Strength and Alloy Content, As- Sintered without Temper**

**Phase II - Alloy Evaluation and Comparison**

The results of the green, sintered, and tensile property testing for P9, P11, SH1, SH2, SH3, and SH4 appear in Table VI.

**Table VI: Alloy Comparison to Existing Sinter-Hardening Materials**

Mix	Comp Press (ksi)	Green Density (g/cm <sup>3</sup> )	Green Strength (psi)	Green Exp (%)	Sintered Density (g/cm <sup>3</sup> )	TRS (psi x 10 <sup>3</sup> )	Dim. Change (%)	Hard (HRC)	YS (psi x 10 <sup>3</sup> )	UTS (psi x 10 <sup>3</sup> )	Elong (%)
P9	30	6.72	1105	0.15	6.64	129	+ 0.19	18	69	71	0.7
	40	6.98	1422	0.20	6.87	158	+ 0.26	20	79	87	0.8
	50	7.11	1884	0.21	7.02	176	+ 0.29	26	86	87	0.8
P11	30	6.64	733	0.19	6.56	88	+ 0.18	36	55	60	0.5
	40	6.92	1081	0.19	6.83	111	+ 0.25	41	62	71	0.5
	50	7.08	1281	0.24	6.99	126	+ 0.28	46	61	87	0.5
SH1	30	6.95	1727	0.20	6.87	143	+ 0.20	22	59	69	0.8
	40	7.12	2216	0.25	7.03	157	+ 0.27	23	64	79	0.9
	50	7.18	2251	0.28	7.12	164	+ 0.33	26	63	80	1.0
SH2	30	6.97	1401	0.20	6.86	152	+ 0.08	20	73	93	1.1
	40	7.13	1659	0.24	7.06	173	+ 0.15	25	84	106	1.2
	50	7.20	1847	0.28	7.15	192	+ 0.19	27	82	102	1.1
SH3	30	6.77	1069	0.17	6.82	141	+ 0.39	4	70	77	0.8
	40	7.15	1610	0.22	7.01	166	+ 0.42	8	78	87	0.9
	50	7.23	1674	0.27	7.11	181	+ 0.46	12	82	94	1.1
SH4	30	6.70	1300	0.15	6.61	111	+ 0.39	22	61	67	0.6
	40	6.95	1493	0.20	6.87	137	+ 0.43	25	0	78	0.6
	50	7.03	1636	0.24	7.02	159	+ 0.45	28	0	89	0.7

\*Note - Mechanical properties, as-sintered without temper

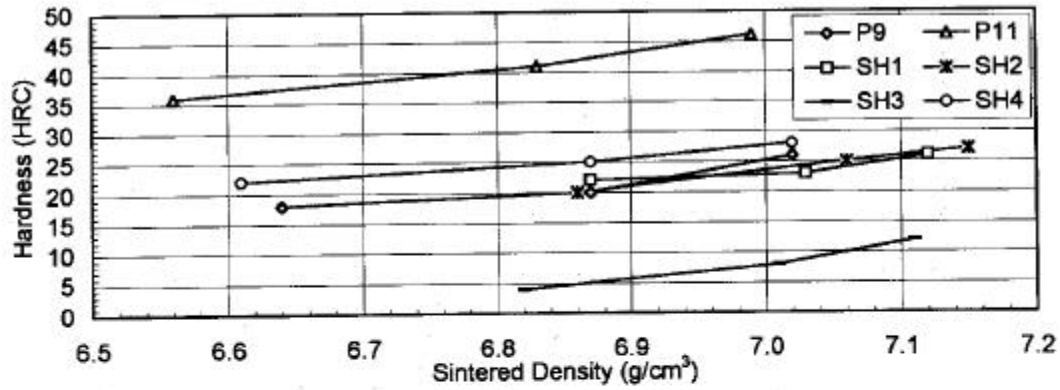


Figure 4: Apparent Hardness as a Function of Sintered Density Sintered under Laboratory Conditions

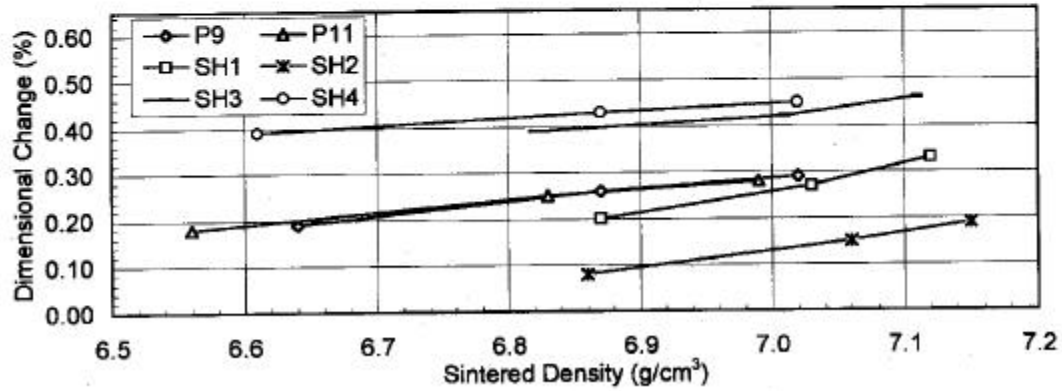


Figure 5: Dimensional Change as Function of Sintered Density Sintered under Laboratory Conditions

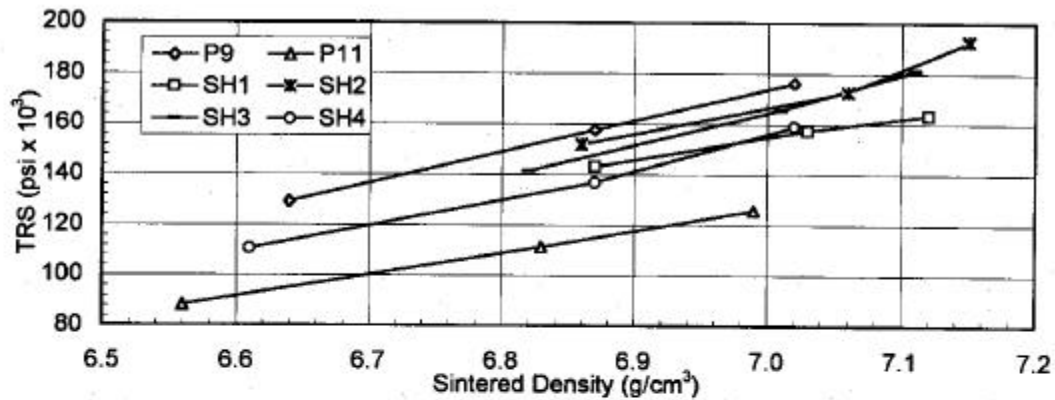


Figure 6: Transverse Rupture Strength as Function of Sintered Density Sintered under Laboratory Conditions

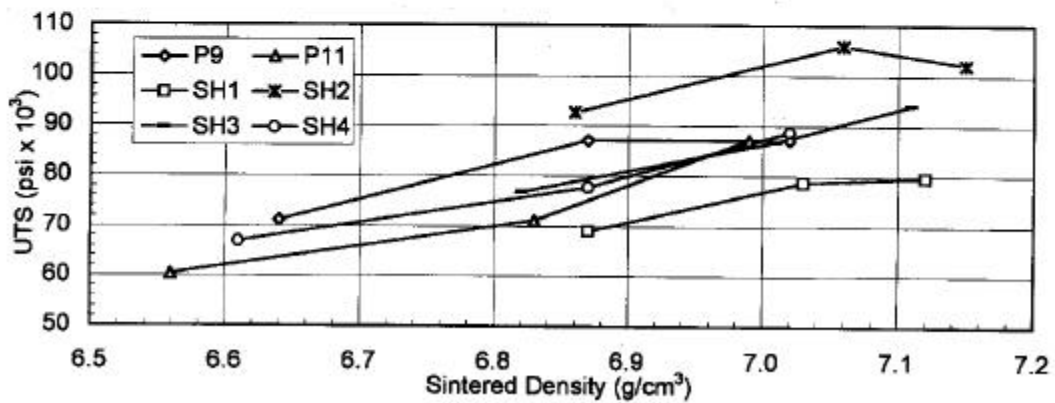


Figure 7: Ultimate Tensile Strength as Function of Sintered Density Sintered under Laboratory Conditions

**Table VII: Sintered Properties of P9, P11, and SH4 Premixes after Tempering at 400°F for 1 Hour**

Mix	Comp Press (tsi)	Green Density (g/cm <sup>3</sup> )	Sintered Density (g/cm <sup>3</sup> )	TRS (psi $\times 10^3$ )	Dim Change (%)	Hard (HRC)	YS (psi $\times 10^3$ )	UTS (psi $\times 10^3$ )	Elong (%)
P9 Tempered	30	6.72	6.66	161	+ 0.17	15	80	84	0.7
	40	6.98	6.90	196	+ 0.21	21	86	103	0.9
	50	7.11	7.04	230	+ 0.26	24	99	117	1.0
P11 Tempered	30	6.64	6.58	164	+ 0.15	27	80	97	0.9
	40	6.92	6.84	214	+ 0.20	32	99	121	1.1
	50	7.08	7.00	240	+ 0.24	36	110	142	1.1
SH4 Tempered	30	6.64	6.57	149	+ 0.16	15	69	83	0.9
	40	6.91	6.83	189	+ 0.24	19	82	102	1.1
	50	7.05	7.00	213	+ 0.28	24	85	116	1.3

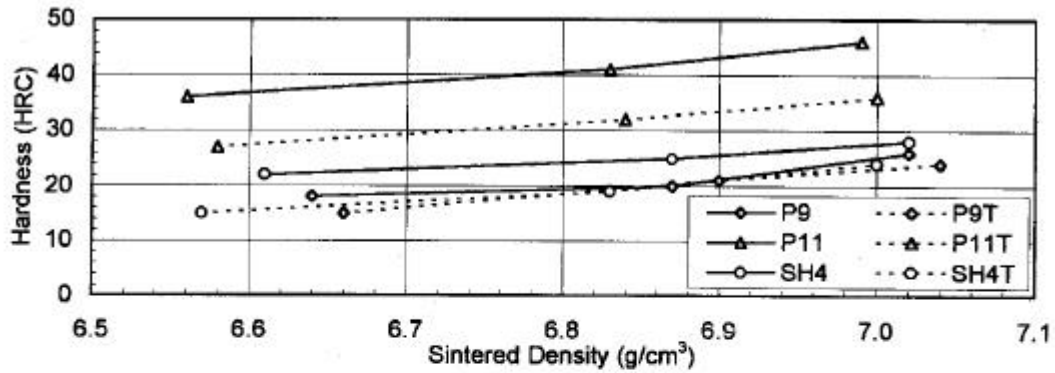


Figure 8: Effect of Tempering on Apparent Hardness of P9, P11, and SH4

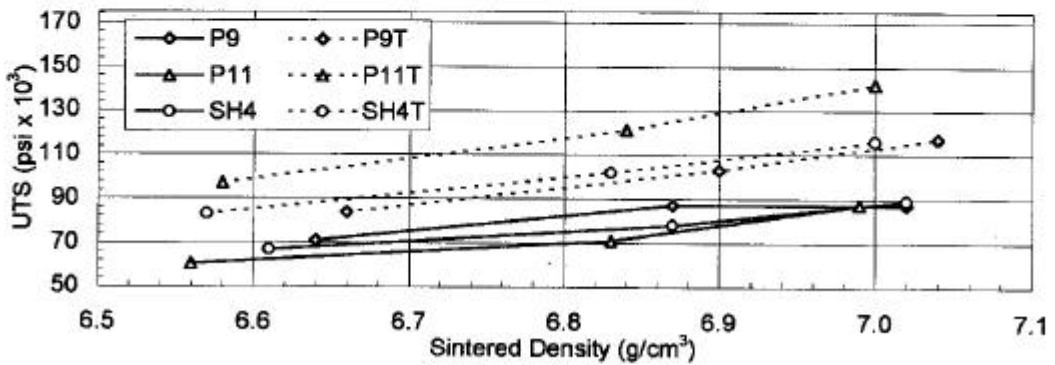
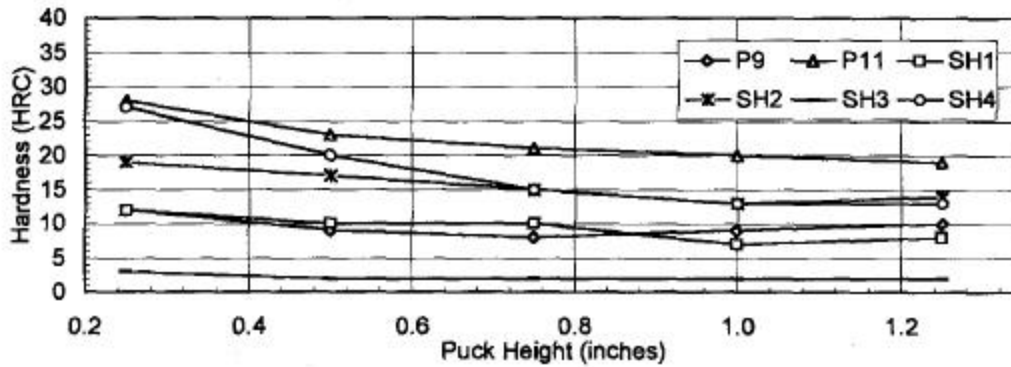


Figure 9: Effect of Tempering on Ultimate Tensile Strength of P9, P11, and SH4

**Table IX: Apparent Hardness Characteristics of Pucks Sintered Under Production Conditions - Standard Cycle (HRC (B)) - As Tempered at 400°F for 1 Hour**

Material	0.25 inch Puck	0.50 inch Puck	0.75 inch Puck	1.00 inch Puck	1.25 inch Puck
P9	12	9	8	9	10
P11	28	23	21	20	19
SH1	12	10	10	7	8
SH2	19	17	15	13	14
SH3	3 (84)	2 (83)	2 (83)	2 (83)	2 (83)
SH4	27	20	15	13	13



**Figure 10: Apparent Hardness as a Function of Puck Height - Standard Cooling Cycle - Tempered at 400°F for 1 Hour**

**Table X: Apparent Hardness Characteristics of Pucks Sintered Under Production Conditions - Sinter-Hardening Cycle (HRC) - Tempered at 400°F for 1 Hour**

Material	0.25 inch Puck	0.50 inch Puck	0.75 inch Puck	1.00 inch Puck	1.25 inch Puck
P9	31	27	26	22	23
P11	34	32	35	34	35
SH1	22	20	23	21	20
SH2	30	26	25	22	23
SH3	20	18	14	13	13
SH4	35	35	34	36	33

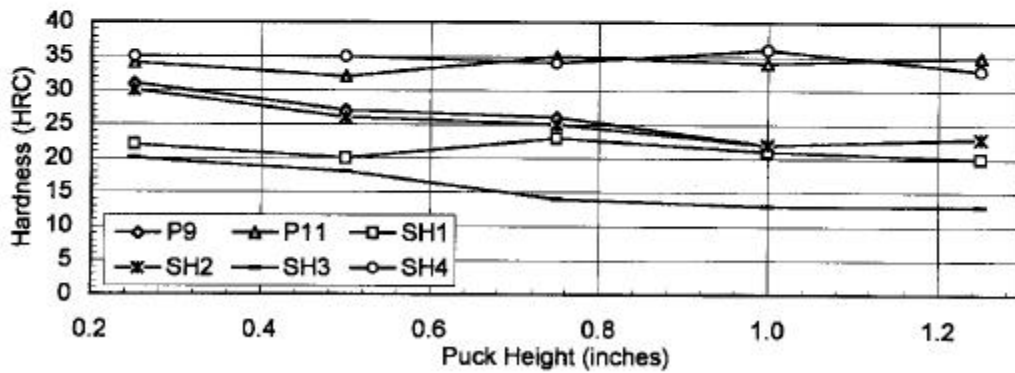


**Figure 11: Apparent Hardness as a Function of Puck Height - Sinter-Hardening Cycle - Tempered at 400°F for 1 Hour**

**Table XI: Martensite Content and Apparent Hardness in the Core of the 1.25 inch Pucks - Sinter-Hardening Cycle - As Tempered at 400°F for 1 Hour**

<b>Material</b>	<b>Hardness on Surface of 1.25 inch Puck (HRC)</b>	<b>Hardness in Core of 1.25 inch Puck (HRC)</b>	<b>Martensite Content Core of 1.250 inch Puck</b>
P9	23	20	25%
P11	35	35	90%
SH1	20	20	49%
SH2	23	21	47%
SH3	13	11	10%
SH4	33	33	81%

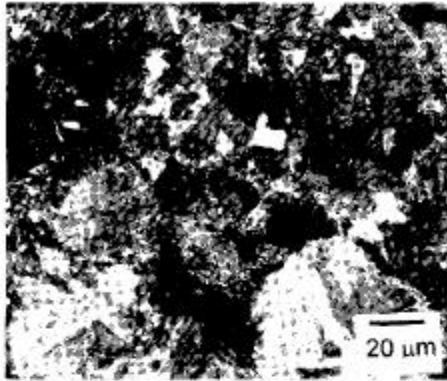


Figure 12: Photomicrograph of P9  
(Original Magnification 500x)

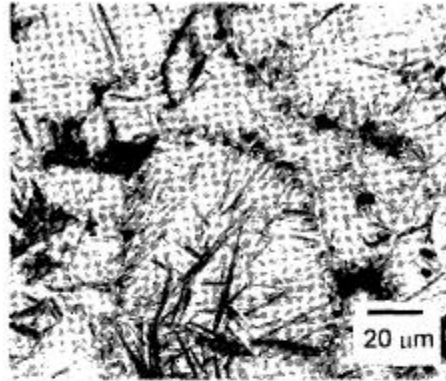


Figure 13: Photomicrograph of P11  
(Original Magnification 500x)

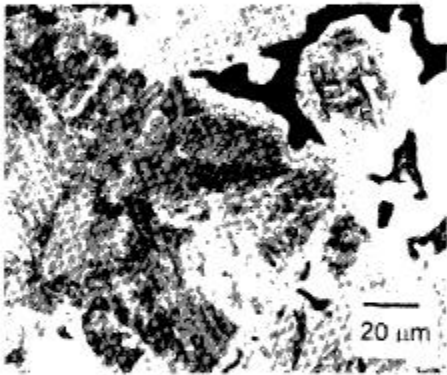


Figure 14: Photomicrograph of SH1  
(Original Magnification 500x)

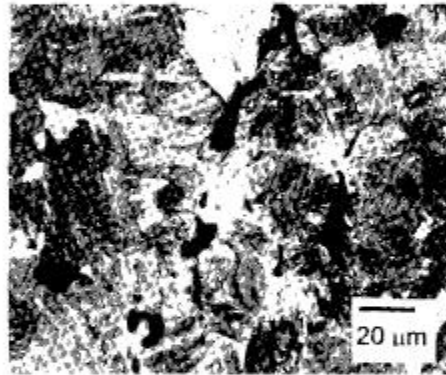


Figure 15: Photomicrograph of SH2  
(Original Magnification 500x)

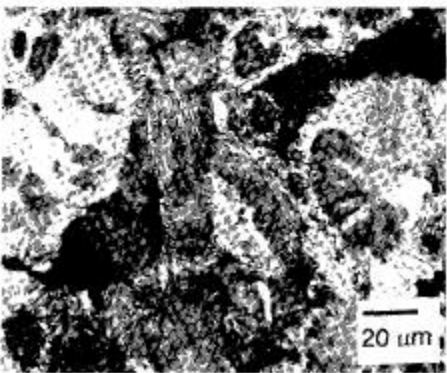


Figure 16: Photomicrograph of SH3  
(Original Magnification 500x)

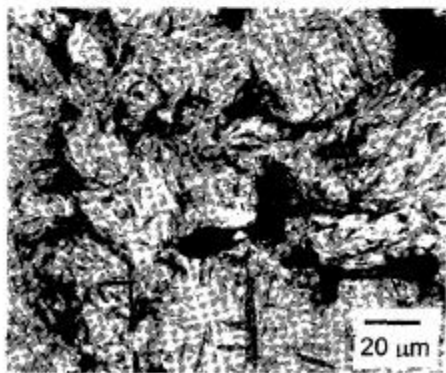
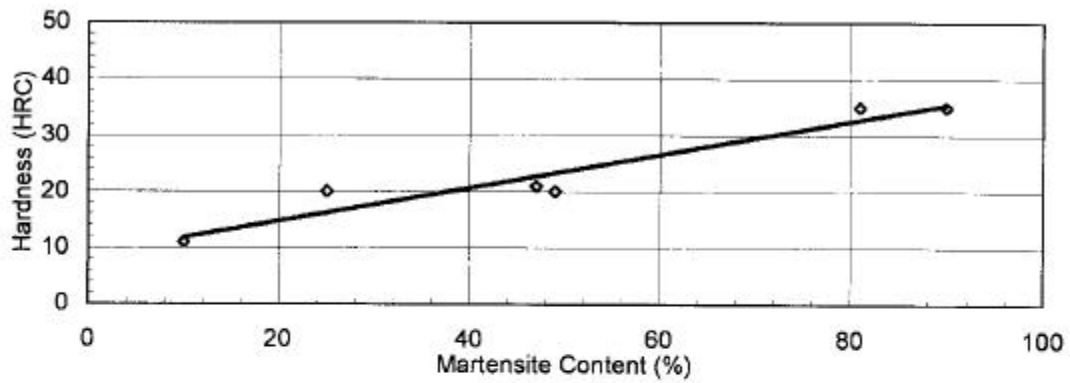
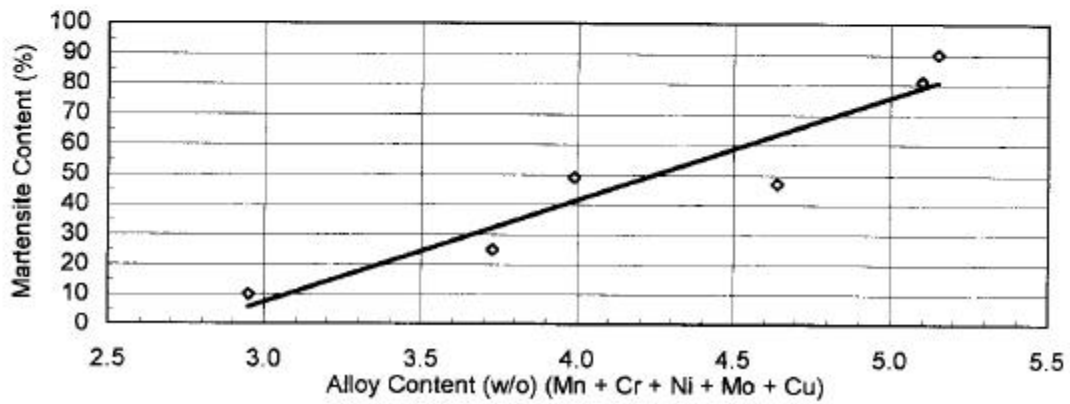


Figure 17: Photomicrograph of SH4  
(Original Magnification 500x)



**Figure 18: Apparent Hardness as a Function of Martensite Content in the Core of the Pucks**



**Figure 19: Martensite Content as a Function of Alloy Content**